



Published in final edited form as:

*Am J Ophthalmol.* 2017 April ; 176: 53–60. doi:10.1016/j.ajo.2017.01.001.

## Relationship Between Central Retinal Vessel Trunk Location and Visual Field Loss in Glaucoma

MENGYU WANG, HUI WANG, LOUIS R. PASQUALE, NEDA BANIASADI, LUCY Q. SHEN, PETER J. BEX, and TOBIAS ELZE

Schepens Eye Research Institute (M.W., H.W., N.B., T.E.), Massachusetts Eye and Ear (L.R.P., L.Q.S.), and Channing Division of Network Medicine, Brigham and Women's Hospital (L.R.P.), Harvard Medical School, Boston, Massachusetts; Institute for Psychology and Behavior, Jilin University of Finance and Economics, Changchun, China (H.W.); Department of Biomedical Engineering and Biotechnology, University of Massachusetts, Lowell, Massachusetts (N.B.); Department of Psychology, Northeastern University, Boston, Massachusetts (P.J.B.); and Max Planck Institute for Mathematics in the Sciences, Leipzig, Germany (T.E.)

### Abstract

**PURPOSE**—To study the relationship between horizontal central retinal vessel trunk location (CRVTL) on glaucomatous optic discs and sector-specific visual field (VF) loss.

**DESIGN**—Retrospective cross-sectional study.

**METHODS**—CRVTL of 421 eyes from 421 patients was manually tracked on the horizontal optic disc axis on fundus images. Focal circumpapillary retinal nerve fiber layer thickness (cpRNFLT) measurements were extracted from optical coherence tomography (OCT). The relationship between focal visual field (VF) loss and CRVTL and focal cpRNFLT was studied by linear regression models. Furthermore, we related central VF loss to CRVTL and focal cpRNFLT separately for mild (VF mean deviation [MD]  $-6$  dB), moderate ( $-12$  dB  $\leq$  MD  $< -6$  dB), and severe (MD  $< -12$  dB) glaucoma.

**RESULTS**—CRVTL nasalization was significantly correlated only to central VF loss (Garway-Heath scheme [central 6 locations, C6]: correlation:  $r = -0.16$ ,  $P < .001$ ; macular vulnerability zone [central 2 locations, C2]:  $r = -0.14$ ,  $P = .003$ ; central 4 locations [C4]:  $r = -0.17$ ,  $P < .001$ ). While focal cpRNFLT at the sectors corresponding to C2 and C6 was significantly correlated to the respective VF sectors as well (C2:  $r = 0.15$ ,  $P = .002$ ; C6:  $r = 0.10$ ,  $P = .03$ ), multivariate models combining cpRNFLT and CRVTL substantially improved structure-function models compared with cpRNFLT alone (likelihood ratio tests, C2 and C6:  $P < .001$ ). The correlations between CRVTL and central VF loss of C4 were  $-0.11$  ( $P = .04$ ),  $-0.39$  ( $P = .01$ ), and  $-0.63$  ( $P = .002$ ) for mild, moderate, and severe glaucoma, respectively.

Inquiries to Tobias Elze, Schepens Eye Research Institute, Harvard Medical School, 20 Staniford St, Boston, MA 02114; tobias-elze@tobias-elze.de.

Supplemental Material available at [AJO.com](http://AJO.com).

**CONCLUSIONS**—CRVTL nasalization is significantly and exclusively correlated to central VF loss for all glaucoma severities independent of cpRNFLT, and thus might be a structural biomarker of central VF loss.

Glaucoma is characterized by optic nerve damage that leads to structural change with accompanying visual field (VF) loss.<sup>1,2</sup> Structure-function modeling provides a construct to understand the onset and progression of glaucoma and has therefore been extensively investigated in previous research.<sup>3–7</sup> For example, retinal nerve fiber layer thickness has been shown to be related to vision loss in glaucoma,<sup>8</sup> and disc tilt has been associated with the location of initial glaucomatous damage.<sup>5</sup>

The relationship between retinal structure and sector-specific VF loss is of particular clinical relevance. The most well-known sectoring scheme for the purpose of mapping retinal damage to sector-specific VF loss was proposed by Garway-Heath and associates.<sup>9</sup> Aside from retinal nerve fiber layer thickness changes, blood vessel positional shift outside the optic nerve head (ONH) has been shown to be associated with glaucoma functional progression.<sup>4</sup> Furthermore, central retinal vessel trunk (ie, the vessel cluster within the ONH) location (CRVTL), which marks the exit position of the retinal vessels on the optic disc, was shown to be associated with spatial patterns of VF loss. In particular, 1 previous study related CRVTL to central VF loss in end-stage glaucoma,<sup>10</sup> while a recent conference abstract reported a higher incidence of temporal VF defects for more temporal CRVTL.<sup>11</sup>

In this work, we quantitatively and systematically study the relationship between sector-specific VF loss and the horizontal CRVTL on the optic disc across the spectrum of glaucoma disease severity.

## METHODS

This retrospective cross-sectional study was approved by the institutional review board (IRB) of Massachusetts Eye and Ear (MEE). The IRB waived the need for informed consent because of the retrospective nature of the study. The study adheres to the Declaration of Helsinki and all federal and state laws.

## PARTICIPANTS AND DATA

Circumpapillary ONH optical coherence tomography (OCT) scans and accompanying VFs (SITA Standard 24-2 protocol) of all patients who presented at MEE glaucoma service between January 2011 and 2014 were initially selected and electronically transferred from the machines (Humphrey Field Analyzer HFA-II and Cirrus HD-OCT, Software version 6.5; Carl Zeiss Meditec AG, Jena, Germany). The initial data selection criteria for VF were fixation loss  $\leq 33\%$ , false-negative rates  $\leq 20\%$ , and false-positive rates  $\leq 20\%$ . The data selection criteria for Cirrus OCT scan (Optic Disc Cube protocol with pixel resolution  $200 \times 200$  within an area of  $6 \text{ mm} \times 6 \text{ mm}$ ) were signal strength  $\geq 6$  and within 1 year from the VF measurement. If more than 1 measurement per eye met the criteria, the most recent measurement was selected. If both eyes of a patient met the selection criteria, only 1 eye was included randomly to avoid potential bias of data samples. As such, we had 2161 pairs of

OCT and VF measurement of 2161 eyes from 2161 patients, which satisfied the criteria of the initial data reliability check.

## DATA PROCESSING

The ONH center is measured using a proprietary technique by the Cirrus OCT machine and then marked on the fundus image. A total of 221 eyes with decentered ONH on OCT scans, defined as OCT scans with ONH centers that deviated more than 0.3 mm in horizontal and vertical direction from the fundus image center, were excluded. OCT fundus images and thickness plots were visually examined by a trained observer for missing thickness data (black pixels on thickness plots) and motion artifacts (defined as vessel shifts of more than 1 vessel diameter or a visible shift within ONH). A total of 167 eyes were excluded because of missing data, and 1082 eyes were excluded owing to motion artifacts. One hundred twenty-two eyes were excluded for missing diagnostic data in the medical record of the respective patient. In addition, we excluded 7 eyes with unidentifiable CRVTL on fundus image owing to low image quality. As our focus was central VF loss induced by glaucoma, we excluded 124 and 17 eyes with cataract (nuclear sclerosis 3+ or worse) and age-related macular degeneration (AMD), respectively. Ultimately, 421 out of 2161 eyes were retained for data analyses.

## CENTRAL RETINAL VESSEL TRUNK LOCATION TRACKING

For CRVTL tracking, we developed a customized software in programming language R (version 3.2.2; R Foundation, Vienna, Austria).<sup>12</sup> In previous work by Huang and associates,<sup>10</sup> CRVTL was defined as the ratio between the distance from CRVT to temporal disc border and the horizontal disc diameter. To take disc torsion into account, we calculated the optimally fitted ellipse around the ONH border (determined by the Cirrus machine based on the OCT volume scan).<sup>13</sup> The fitted ellipse centered at the ONH center was parameterized by major axis, minor axis, and rotation angle. Nonlinear optimization<sup>14</sup> was applied to obtain the optimal fitted ellipse by minimizing the boundary discrepancy between the ellipse and ONH. A trained observer marked the CRVTL on the minor axis (temporal-nasal direction) of the ellipse on each fundus image, as shown in Figure 1. The CRVTL on minor axis was normalized into the range between 0 (temporal pole) and 1 (nasal pole) of the ellipse.

## STATISTICAL ANALYSES

All statistical analyses were performed using the R platform.<sup>12</sup> We applied 2 different VF sectoring schemes and calculated the correlation between CRVTL and average pattern deviation (PD) of each VF sector. The usage of PD was motivated by our intention to emphasize visual sensitivity within each sector relative to the general height of vision. The 2 sectoring schemes of VF encompass the well-known Garway-Heath scheme<sup>9</sup> and our annular scheme, as illustrated in Figure 2 (Left and Right, respectively). The motivation to use an annular scheme was to test whether CRVTL is only associated with central VF loss rather than peripheral VF loss, since temporal CRVTL has been shown to be related to the preservation of central VF loss in end-stage glaucoma.<sup>10</sup> The Garway-Heath scheme was additionally tested because temporal VF defects were related to temporal CRVTL,<sup>11</sup> suggesting that the association of CRVTL with VF loss might reach beyond pure center-

periphery differences. *P* values of the correlations for each sector were corrected for multiple comparisons.<sup>15</sup>

For the sectors for which CRVTL was significantly correlated to the sector VF loss, we evaluated the relationship between focal circumpapillary retinal nerve fiber layer thickness (cpRNFLT), which was mapped to the specific sector of VF in established works,<sup>16,9</sup> and the corresponding sector VF loss. In addition, multivariate analyses were performed to assess whether focal cpRNFLT and CRVTL were independently correlated to the corresponding sector VF loss. Lastly, we performed a correlation test for mild (including suspects) (mean deviation [MD]  $-6$  dB), moderate ( $-12$  dB  $\leq$  MD  $< -6$  dB), and severe (MD  $< -12$  dB) glaucoma, respectively.<sup>17</sup> Our definition of mild glaucoma includes VFs with non-negative MD, as relative differences of light sensitivity between center and periphery, captured by PD values, may be present over the whole MD range, including VFs with normal and supernormal MD. Particularly the group that we called “mild glaucoma” is expected to contain a substantial number of glaucoma suspects in addition to true glaucoma patients.

## RESULTS

TABLE 1 shows the demographics and diagnostic details for the 421 patients satisfying our data selection criteria, and the distribution of mild, moderate and severe glaucoma patients.

Figure 2 shows the correlations between CRVTL and each sector VF loss for the Garway-Heath scheme (Figure 2, Left) and annular scheme (Figure 2, Right). For each sectoring scheme, sectors with average PDs that are significantly correlated ( $P < .05$ ) to CRVTL after *P* value adjustment for multiple comparisons are annotated with the numerical *P* values. The average PDs only of the central sectors from both the Garway-Heath scheme ( $r = -0.16$ ,  $P = .004$ ) and annular scheme ( $r = 0.17$ ,  $P = .002$ ) were significantly correlated to CRVTL, respectively. Moreover, the correlation between the VF loss of the sectors from the annular scheme became monotonically weaker with increasing eccentricity from fixation ( $r = 0.96$ ,  $P = .04$ ), which implies a radial fade-out pattern of the correlation strength between CRVTL and the spatial sector VF loss.

Given the strong and exclusive correlation between CRVTL and central VF loss, we studied the relationship between CRVTL and central VF loss using 3 central VF sectoring approaches, including the 4 most central VF locations (C4) from our annular scheme, the 6 central VF locations (C6) from the Garway-Heath scheme, and the 2 central VF locations (C2) from the macular vulnerability zone proposed by Hood and associates.<sup>16</sup>

As shown in Figure 3, the C6 and C2 central VF sectoring schemes were defined by mappings of retinal nerve fiber trajectories to VF locations.<sup>9,16</sup> As zero angular position was defined as horizontal line toward temporal direction with angular location calculated clockwise, the regions of retinal nerve fiber layer mapped to C6 and C2 are a 89-degree zone from 311 degrees to 40 degrees and a 27-degree zone from 295 degrees to 322 degrees on the peripapillary 1.73-mm standard circle on the Cirrus machine, respectively. For the purpose of comparison, we also evaluated the correlations between the focal cpRNFLT of the corresponding circumpapillary region on the circle around ONH and the VF loss of C6

and C2. The correlations between CRVTL and the VF loss of C4, C6, and C2 were  $-0.17$  ( $P < .001$ ),  $-0.16$  ( $P < .001$ ), and  $-0.14$  ( $P < .003$ ), respectively. The focal cpRNFLT of the circumpapillary region on the peripapillary circle was significantly correlated to the average sector PDs of C6 ( $r = 0.10$ ,  $P = .03$ ) and C2 ( $r = 0.15$ ,  $P = .002$ ), respectively.

Furthermore, we studied by multivariate analyses with the regressors CRVTL and focal cpRNFLT whether the correlation between CRVTL and central VF loss of C6 and C2 was independent of or confounded by focal cpRNFLT. The multivariate linear regression analyses show CRVTL to be independently correlated to the VF loss of C6 and C2 (likelihood ratio tests,  $P < .001$  for both) even after adjustment for the focal cpRNFLT, respectively. The multivariate models combining the focal cpRNFLT and CRVTL substantially improved the structure-function models for C6 and C2 compared with focal cpRNFLT alone, which indicates that cpRNFLT and CRVTL explain different proportions of central VF loss variance. The regression coefficients from the focal cpRNFLT and CRVTL to central VF loss of C6 were  $0.02$  ( $P = .006$ ) and  $3.64$  ( $P < .001$ ), respectively. The regression coefficients from the focal cpRNFLT and CRVTL to central VF loss of C2 were  $0.04$  ( $P < .001$ ) and  $-5.32$  ( $P < .001$ ), respectively.

Figure 4 shows the linear regressions characterizing the negative correlations between CRVTL and central VF loss of C4 for mild ( $r = -0.11$ ,  $P = .04$ ), moderate ( $r = -0.39$ ,  $P = .01$ ), and severe glaucoma ( $r = -0.63$ ,  $P = .002$ ), respectively. In other words, more nasalized CRVTL within the ONH was correlated to lower average PD for the 4 central points (within 3 degrees around fixation) of the Humphrey VF. The correlation strengths between CRVTL and central VF loss in both moderate ( $P = .04$ ) and severe ( $P = .005$ ) glaucoma were significantly stronger than in mild glaucoma.

Table 2 shows the statistical results of linear regressions from CRVTL/cpRNFLT to central VF loss for mild, moderate, and severe glaucoma, respectively. Adding CRVTL as an additional structural parameter significantly improved the structure-function model of the cpRNFLT–central VF loss association for mild ( $P = .003$ ), moderate ( $P = .04$ ), and severe glaucoma ( $P = .047$ ) with the Hood central VF sectoring scheme (C2), and moderate ( $P = .01$ ) and severe ( $P < .001$ ) glaucoma with the Garway-Heath scheme (C6).

Finally, we analyzed the relationship between CRVTL and glaucoma-related parameters as well as myopia. Although CRVTL was significantly correlated to RNFLT on the Cirrus standard circle ( $r = -0.11$ ,  $P = .02$ ), it was not significantly correlated to MD ( $r = 0.02$ ,  $P = .75$ ). Moreover, there was no significant group difference of CRVTL between those VFs with glaucoma hemifield test within normal limits ( $0.593 \pm 0.122$ ) and outside normal limits ( $0.590 \pm 0.124$ ), as confirmed by  $t$  test<sup>18</sup> ( $P = .78$ ). Though spherical equivalent of refractive error was significantly correlated to CRVTL ( $r = -0.30$ ,  $P < .001$ ), it was not significantly correlated to central VF loss ( $r = 0.01$ ,  $P = .92$ ).

## DISCUSSION

We evaluated the correlations between crvttl and the sector-specific VF loss in 2 different sectoring schemes: the Garway-Heath scheme and our annular scheme. In addition, the

correlation between CRVTL and the central VF loss in the Hood macular vulnerability zone scheme was assessed. We found CRVTL nasalization to be significantly correlated to central VF loss for the whole range of glaucoma severity. The correlation strengths in moderate and severe glaucoma were significantly stronger than in mild glaucoma. Our novel clinical finding might potentially improve the understanding of the pathologic vascular mechanisms underlying central VF loss in glaucoma. Moreover, the correlations between CRVTL and central VF loss were significantly independent of the focal cpRNFLT of the RNF layer region mapped to the central VF locations illustrated by likelihood ratio test. Therefore, a multivariate model combining CRVTL and the focal RNFLT will improve the structure-function modeling in glaucoma.

We observed that the correlation strengths between CRVTL and central VF loss of C4 in moderate ( $P = .04$ ) and severe ( $P = .005$ ) glaucoma were significantly stronger than in mild glaucoma. There was no significant correlation strength difference ( $P = .13$ ) between moderate and severe glaucoma. Note that CRVTL itself was not significantly correlated to MD ( $r = 0.02$ ,  $P = .74$ ), which might suggest that CRVTL nasalization is not necessarily the result of glaucoma progression but rather a stable anatomic parameter that acts as a risk factor to develop central VF loss in the course of glaucoma. Longitudinal studies are needed to clarify this issue. If this were the case, it would explain the weaker correlation between CRVTL and central VF loss in mild glaucoma because many patients in the mild glaucoma group were just glaucoma suspects and had normal visual function.

It has previously been suggested that retinal structural changes are better correlated to functional measures expressed in linear scale rather than the logarithmic decibel scale used by the HFA device,<sup>19–22</sup> although standard summary indices like MD, which is used in many studies, are also calculated on the original logarithmic scale. To rule out that our correlation between CRVTL and central VF loss was confounded by the logarithmic PD scale, we repeated our data analysis after transforming the PD values to a linear scale before averaging<sup>21,22</sup> and observed a similar relationship ( $r = -0.16$ ,  $P = .001$ ).

Our study was inspired by 2 previously proposed theories. First, CRVTL is related to the preservation of central island vision for severe glaucoma, which was shown by Huang and associates.<sup>10</sup> In our study, we have shown that the correlation between CRVTL and central VF loss is not restricted to severe glaucoma, and CRVTL is also significantly correlated to central VF loss in mild and moderate glaucoma. A previous study<sup>23</sup> also has shown that nasalized CRVTL was related to thinner temporal RNFLT. However, since nasalized CRVTL is also associated with more temporal retinal vessel trajectories outside the ONH that correspond to the RNFLT peak, it cannot be distinguished whether the observed thinning of temporal RNFLT was attributable to pathologic cause or anatomic variation. A recent study<sup>24</sup> using lateral scans of swept-source OCT has shown that peripheral CRVTL was associated with larger lamina cribrosa surface depth and thinner global RNFLT and inferred that CRVTL may contribute to the resistance of the lamina cribrosa against deformation. In agreement with this, we also observed the correlation between CRVTL and RNFLT on the Cirrus standard circle ( $r = -0.11$ ,  $P = .02$ ). However, it cannot be inferred from our cross-sectional data whether RNFLT thinning is a causal factor. Second, our study was also inspired by the theory of mapping the central visual field to cpRNFLT. The theory is

summarized by Hood and associates.<sup>25</sup> The mapping between macular vulnerability zone and focal cpRNFL was established for early glaucoma only. To our best knowledge, we are the first to show that CRVTL as a structural biomarker is correlated to central VF loss over the whole range of glaucoma severity, and moreover, that this relationship is independent of focal cpRNFL.

In our study, we used PD to measure focal VF loss. The PD plot quantifies focal visual deficits after subtracting out the general reduction of retinal sensitivity across the island of vision. Therefore, small focal VF deviations in early glaucoma stages, even in the presence of non-negative MD, are highlighted. At the same time, PDs highlight central islands in severe glaucoma by positive values even though the corresponding total deviation values might be strongly negative.

We would like to emphasize that adding CRVTL as an additional structural parameter improves the structure-function correlation compared with the model of central VF loss based on cpRNFLT alone, which is the status quo of structure-function modeling of central VF loss. Based on our results, CRVTL significantly improves the structure-function model of the cpRNFLT–central VF loss for all severity groups with the Hood central VF sectoring scheme (C2) and for moderate and severe groups with the Garway-Heath scheme (C6). In addition, there were no significant correlations between central VF loss and the cpRNFLT for each glaucoma subgroup for both the Garway-Heath and Hood central VF sectoring schemes, whereas CRVTL was significantly correlated to central VF loss in moderate and severe glaucoma for the Garway-Heath central VF sectoring schemes (C6) and significantly correlated to central VF loss in mild glaucoma for the Hood central VF sectoring schemes (C2).

There are 2 potential pathologic interpretations for the association between CRVTL and central VF loss. First, the CRVT may act as a stabilization support preventing glaucomatous deformations in the lamina cribrosa. Nasalized CRVTL will result in less mechanical support for lamina cribrosa in the temporal region, which is thus more susceptible to glaucomatous damages. Second, nasalized CRVTL may affect the adequacy of vascular supply in the temporal region, leading to thinning of RNFL in the macular region.

Whereas in most previous studies the optic disc border was manually traced on the fundus photographs, in our work the disc border was automatically segmented by the Cirrus machine based on the Bruch membrane opening<sup>26</sup> identified on the 3-dimensional OCT volume scans, which promises a more objective disc segmentation compared with the 2-dimensional fundus images.

This study has several limitations. Our cross-sectional design cannot determine whether CRVTL nasalization is a causative factor for central VF loss or the consequence of central VF loss. Prospective studies are needed to clarify this issue. Because Humphrey VF 24-2 undersamples the visual function in the central VF, specific central VF tests such as Humphrey VF 10-2 will be needed to better characterize the relationship between central VF and CRVTL. In addition, our work did not incorporate data on nonocular factors previously reported to be associated with central VF loss, including cellular<sup>27</sup> (eg, soluble guanylyl

cyclase), genomic<sup>27–29</sup> (eg, CAV1/CAV2, single nucleotide polymorphisms, and p53 region), and health habit factors<sup>30,31</sup> (eg, body mass index, smoking, and eating leafy green vegetables), with our retinal anatomic features (eg, CRVTL and focal RNFLT) to better predict central VF loss. Finally, the definition of CRVTL is another limitation, because the viewing angle used for ONH imaging can also affect the accuracy of CRVTL measurement.

To summarize, our results, based on a large sample of over 400 eyes from a clinical glaucoma service, show that a more nasal location of the central retinal vessel trunk is significantly correlated to central VF loss. CRVTL nasalization might therefore be a structural biomarker of central VF loss in glaucoma.

## Supplementary Material

Refer to Web version on PubMed Central for supplementary material.

## Acknowledgments

FUNDING/SUPPORT: This work was supported by the Massachusetts Lions Eye Research Fund, Belmont, Massachusetts (M.W., N.B., T.E.), the Grimshaw-Gudewicz Foundation, Fall River, Massachusetts (M.W., N.B., T.E.), NIH grant R01 EY018664 (T.E., P.J.B.), Harvard Glaucoma Center of Excellence, Boston, Massachusetts (T.E., L.R.P., L.Q.S.), China Scholarship Council, Beijing, China (H.W.), and The Eleanor and Miles Shore Fellowship, Harvard Medical School, Boston, Massachusetts (L.Q.S.). Financial Disclosures: Peter J. Bex and Tobias Elze: patent (WO2015027225 A1). The following authors have no financial disclosures: Mengyu Wang, Hui Wang, Louis R. Pasquale, Neda Baniasadi, and Lucy Q. Shen. All authors attest that they meet the current ICMJE criteria for authorship.

## References

1. Rossetti L, Digiuni M, Giovanni M, et al. Blindness and glaucoma: a multicenter data review from 7 academic eye clinics. *PLoS One*. 2015; 10(8):e0136632. [PubMed: 26302445]
2. Mermoud A. Glaucoma is second leading cause of blindness globally. *Bull World Health Organ*. 2004; 82:887–888. [PubMed: 15640929]
3. Pollet-Villard F, Chiquet C, Romanet JP, Noel C, Aptel F. Structure-function relationships with spectral-domain optical coherence tomography retinal nerve fiber layer and optic nerve head measurements. *Invest Ophthalmol Vis Sci*. 2014; 55(5):2953–2962. [PubMed: 24692125]
4. Radcliffe NM, Smith SD, Syed ZA, et al. Retinal blood vessel positional shifts and glaucoma progression. *Ophthalmology*. 2014; 121(4):842–848. [PubMed: 24342023]
5. Choi JA, Park HYL, Shin HY, Park CK. Optic disc tilt direction determines the location of initial glaucomatous damage. *Invest Ophthalmol Vis Sci*. 2014; 55(8):4991–4998. [PubMed: 24985480]
6. Anton A, Yamagishi N, Zangwill L, Sample A, Weinreb RN. Mapping structural to functional damage in glaucoma with standard automated perimetry and confocal scanning laser ophthalmoscopy. *Am J Ophthalmol*. 1998; 125(4):436–446. [PubMed: 9559728]
7. Medeiros FA, Leite MT, Zangwill LM, Weinreb RN. Combining structural and functional measurements to improve detection of glaucoma progression using Bayesian hierarchical models. *Invest Ophthalmol Vis Sci*. 2011; 52(8):5794–5803. [PubMed: 21693614]
8. El Beltagi TA, Bowd C, Boden C, et al. Retinal nerve fiber layer thickness measured with optical coherence tomography is related to visual function in glaucomatous eyes. *Ophthalmology*. 2003; 110(11):2185–2191. [PubMed: 14597528]
9. Garway-Heath DF, Poinoosawmy D, Fitzke FW, Hitchings RA. Mapping the visual field to the optic disc in normal tension glaucoma eyes. *Ophthalmology*. 2000; 107(10):1809–1815. [PubMed: 11013178]



10. Huang H, Jonas JB, Dai Y, et al. Position of the central retinal vessel trunk and pattern of remaining visual field in advanced glaucoma. *Br J Ophthalmol*. 2013; 97(1):96–100. [PubMed: 23125065]
11. Besombes G, Grunewald F, Ramdane N, Salleron J, Labalette P, Rouland JF. Position of the central retinal vessel trunk and location of visual field and parapapillary nerve fibers damage in early to moderate glaucoma. *Invest Ophthalmol Vis Sci*. 2014; 55(13):950.
12. The R Core Team R: A Language and Environment for Statistical Computing. Vienna, Austria: R Foundation for Statistical Computing; 2014.
13. Park HYL, Lee K, Park CK. Optic disc torsion direction predicts the location of glaucomatous damage in normal-tension glaucoma patients with myopia. *Ophthalmology*. 2012; 119(9):1844–1851. [PubMed: 22595297]
14. Nelder JA, Mead R. A simplex method for function minimization. *Comput J*. 1965; 7(4):308–313.
15. Benjamini Y, Hochberg Y. Controlling the false discovery rate: a practical and powerful approach to multiple testing. *J R Statist Soc B*. 1995:289–300.
16. Hood DC, Raza AS, de Moraes CGV, et al. Initial arcuate defects within the central 10 degrees in glaucoma. *Invest Ophthalmol Vis Sci*. 2011; 52(2):940–946. [PubMed: 20881293]
17. Hodapp, E., Parrish, RK., Anderson, DR. *Clinical Decisions in Glaucoma*. St Louis, MO: Mosby Inc; 1993.
18. Kendall, MG., Stuart, A., Ord, J. *The Advanced Theory of Statistics*. Vol. 3. London: Charles Griffin; 1968.
19. Harwerth RS, Carter-Dawson L, Smith EL 3rd, Barnes G, Holt WF, Crawford ML. Neural losses correlated with visual losses in clinical perimetry. *Invest Ophthalmol Vis Sci*. 2004; 45(9):3152–3160. [PubMed: 15326134]
20. Harwerth R, Wheat J, Fredette M, Anderson DR. Linking structure and function in glaucoma. *Prog Retin Eye Res*. 2010; 29(4):249–271. [PubMed: 20226873]
21. Hood DC, Anderson SC, Wall M, Kardon RH. Structure versus function in glaucoma: an application of a linear model. *Invest Ophthalmol Vis Sci*. 2007; 48(8):3662–3668. [PubMed: 17652736]
22. Hood DC, Kardon RH. A framework for comparing structural and functional measures of glaucomatous damage. *Prog Retin Eye Res*. 2007; 26(6):688–710. [PubMed: 17889587]
23. Jonas JB, Budde WM, Németh J, Gründler AE, Mistlberger A, Hayler JK. Central retinal vessel trunk exit and location of glaucomatous parapapillary atrophy in glaucoma. *Ophthalmology*. 2001; 108(6):1059–1064. [PubMed: 11382629]
24. Oh BL, Lee EJ, Kim H, Girard MJ, Mari JM, Kim TW. Anterior lamina cribrosa surface depth in open-angle glaucoma: Relationship with the position of the central retinal vessel trunk. *PLoS One*. 2016; 11(6):e0158443. [PubMed: 27355646]
25. Hood DC, Raza AS, de Moraes CGV, Liebmann JM, Ritch R. Glaucomatous damage of the macula. *Prog Retin Eye Res*. 2013; 32:1–21. [PubMed: 22995953]
26. Carl Zeiss Meditec, Inc. CIRRUS User Manual 6.0.2 User Manual. Jena Germany: Carl Zeiss Meditec, Inc; 2012.
27. Buys ES, Ko YC, Alt C, et al. Soluble guanylate cyclase 1-deficient mice: a novel murine model for primary open angle glaucoma. *PLoS One*. 2013; 8(3):e60156. [PubMed: 23527308]
28. Wiggs JL, Hewitt AW, Fan BJ, et al. The p53 codon 72 pro/pro genotype may be associated with initial central visual field defects in caucasians with primary open angle glaucoma. *PLoS One*. 2012; 7(9):e45613. [PubMed: 23049825]
29. Loomis SJ, Kang JH, Weinreb RN, et al. Association of *cav1/cav2* genomic variants with primary open-angle glaucoma overall and by gender and pattern of visual field loss. *Ophthalmology*. 2014; 121(2):508–516. [PubMed: 24572674]
30. Kang JH, Loomis SJ, Rosner BA, et al. Comparison of risk factor profiles for primary open-angle glaucoma subtypes defined by pattern of visual field loss: a prospective study. *Invest Ophthalmol Vis Sci*. 2015; 56(4):2439–2448. [PubMed: 25758813]
31. Kang JH, Willett WC, Rosner BA, Buys E, Wiggs JL, Pasquale LR. Association of dietary nitrate intake with primary open-angle glaucoma: a prospective analysis from the nurses' health study and

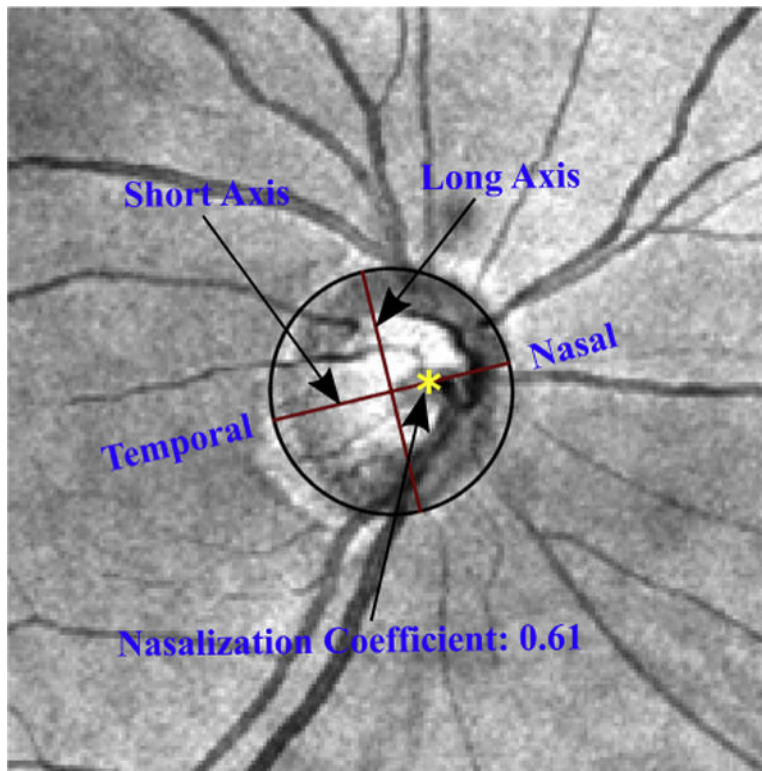
health professionals follow-up study. *JAMA Ophthalmol.* 2016; 134(3):294–303. [PubMed: 26767881]

Author Manuscript

Author Manuscript

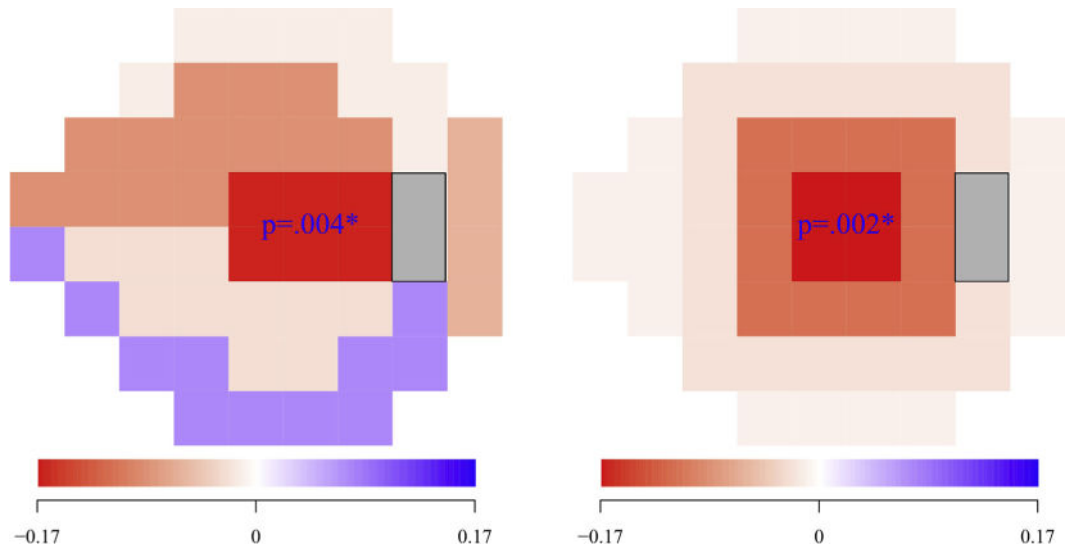
Author Manuscript

Author Manuscript



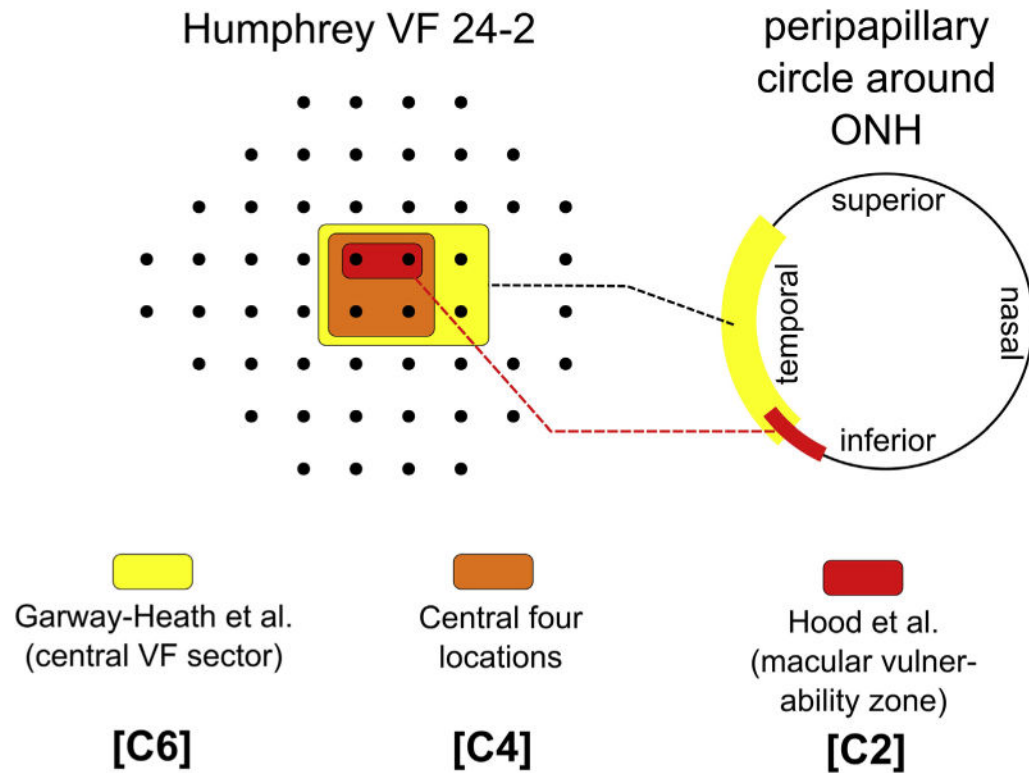
**FIGURE 1.**

Example of fundus image with optimally fitted ellipse and central retinal vessel trunk location (CRVTL) marked by a trained observer (yellow asterisk). The ellipse was fitted around the optic nerve head (ONH) border segmented by optical coherence tomography (not shown here) and overlaid on the fundus image for illustrative purposes. For CRVTL tracking, only the direction of the long axis was displayed. Ellipse borders were not visible to the observer.

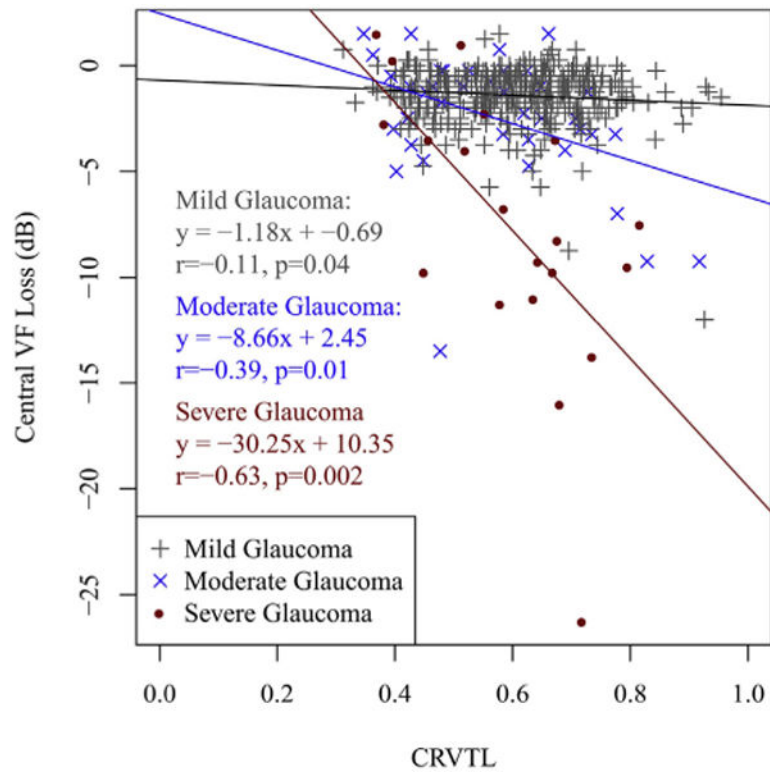


**FIGURE 2.**

Correlation between central retinal vessel trunk location (CRVTL) and the average pattern deviations (PDs) of different sectors of visual field (VF) for the (Left) Garway-Heath scheme and (Right) annular scheme. For each VF sectoring scheme, sectors with correlations that are significant ( $P$  values of correlations are marked by asterisk).



**FIGURE 3.** Schematic of C4, C6, and C2 central visual field (VF) sectoring scheme on 24-2 Humphrey VF. The retinal nerve fiber layer regions mapped to C6 and C2 on the peripapillary circle (1.73 mm around optic nerve head [ONH]) are annotated with yellow and dark red colors, respectively. C4, C6, and C2 refer to the 4, 6, and 2 most central VF locations from our annular scheme, the Garway-Heath scheme, and the macular vulnerability zone proposed by Hood and associates,<sup>16</sup> respectively.

**FIGURE 4.**

Linear regressions from central retinal vessel trunk location (CRVTL) to central visual field (VF) loss of C4 for mild glaucoma ( $r = -0.11$ ,  $P = .04$ ), moderate glaucoma ( $r = -0.39$ ,  $P = .01$ ), and severe glaucoma ( $r = -0.63$ ,  $P = .002$ ), respectively. C4 refers to the 4 most central VF locations from our annular scheme.

Descriptive Statistics of the Demographics and Detailed Diagnostics of the Glaucoma Patients Obtained From the Medical Patient Records

TABLE 1

Race	European	308	Asian	31	African	46	Hispanic	20	Mixed/Other	16
Glaucoma Type	OAG	189	ACG	5	MMG	9	Suspects	218		
Glaucoma Severity <sup>a</sup>	Mild	361	Moderate	39	Severe	21				
Basic Descriptive Statistics	Age	59.0 ± 13.0	Sex (M/F)	196/225	MD (dB)	-3.0 ± 4.2				

ACG = angle closure glaucoma (primary or secondary); MD = mean deviation; MMG = mixed mechanism glaucoma; OAG = open-angle glaucoma (primary or secondary).

<sup>a</sup>Mild glaucoma: MD -6 dB; moderate glaucoma: -12 dB MD < -6 dB; severe glaucoma: MD < -12 dB.

**TABLE 2**

Descriptive Statistics of the Results of Linear Regressions From Central Retinal Vessel Trunk Location/ Circumpapillary Retinal Nerve Fiber Layer Thickness to Central Visual Field Loss for Mild, Moderate, and Severe Glaucoma Groups

CVFL Sectoring Approach	Result Variable	Mild Glaucoma	Moderate Glaucoma	Severe Glaucoma
C6 (Garway-Heath)	CVFL	-1.57 ± 1.13	-2.74 ± 3.25	-7.30 ± 6.50
	r <sub>CRVTL</sub> ( <i>P</i> value)	-0.08 (.11)	-0.38 (.02*)	-0.65 (.002*)
	r <sub>cpRNFLT</sub> ( <i>P</i> value)	0.05 (.36)	-0.08 (.62)	-0.13 (.56)
	Improvement by CRVTL (LRT <i>P</i> value)	.08	.01*	<.001*
C2 (Hood)	CVFL	-1.53 ± 1.88	3.51 ± 5.58	-10.14 ± 9.80
	r <sub>cpRNFLT</sub> ( <i>P</i> value)	-0.14 (.008*)	0.28 (.08)	-0.42 (.055)
	r <sub>cpRNFLT</sub> ( <i>P</i> value)	0.09 (.06)	0.04 (.78)	0.12 (.59)
	Improvement by CRVTL (LRT <i>P</i> value)	.003*	.04*	.047*

cpRNFLT = circumpapillary retinal nerve fiber layer thickness; CRVTL = central retinal vessel trunk location; CVFL = central visual field loss; LRT = likelihood ratio test; VF = visual field.

LRT demonstrates whether adding CRVTL as additional structural parameter improves the structure-function model of the cpRNFLT–central VF association. Significant results ( $P < .05$ ) are marked by asterisks. C6 and C2 refer to the 6 and 2 most central VF locations from the Garway-Heath scheme<sup>9</sup> and the macular vulnerability zone proposed by Hood and associates,<sup>16</sup> respectively.